Influence of a one-neutron-excess projectile on low-energy incomplete fusion

Vijay R. Sharma,[1,*] Abhishek Yadav,[1] Pushpendra P. Singh,[2] Devendra P. Singh,[1] Sunita Gupta,[3] M. K. Sharma,[4] Indu Bala,[5] R. Kumar,[5] S. Murlithar,[5] B. P. Singh,[1,†] and R. Prasad[1]

[1]*Accelerator Laboratory, Physics Department, A. M. University, Aligarh 202 002, India*
[2]*Department of Physics, Indian Institute of Technology Ropar, Punjab 140 001, India*
[3]*Physics Department, Agra College, Agra 282 001, India*
[4]*Physics Department, S. V. College, Aligarh 202 001, India*
[5]*NP-Group, Inter-University Accelerator Centre, New Delhi 110 067, India*

(Received 15 August 2013; revised manuscript received 2 December 2013; published 18 February 2014)

Background: Incomplete fusion has been found to be an important contributor in light heavy-ion ($A \leqslant 20$) induced reactions even at slightly above barrier energies.
Purpose: For better insight into the dynamics of incomplete fusion, the onset and influence of incomplete fusion need to be investigated in terms of projectile energy ($E_{\rm lab}$) and entrance channel mass-asymmetry (μ_A). A rich set of experimental data on incomplete fusion may be useful to correlate the probability of incomplete fusion with the various entrance channel parameters and eventually to develop a theoretical model code for the same. Presently, there is no theoretical model available which can explain low-energy incomplete fusion data consistently.
Methods: The excitation functions of complete and incomplete fusion residues populated in the ^{13}C+^{169}Tm system have been measured using the recoil-catcher activation technique followed by offline γ spectroscopy. The evaporation residues have been identified on the basis of characteristic γ lines and confirmed through the decay-curve analysis.
Results: The excitation functions of xn and pxn channels are found to be in good agreement with the statistical model code PACE4; this suggests the population of these channels via complete fusion. Some residues are found to have a contribution from their higher charge isobar precursor decay. The precursor contribution has been deduced from the cumulative cross section using the standard successive radioactive decay formulations. The excitation functions of α-emitting channels are observed to be significantly enhanced as compared to the statistical model code PACE4. This enhancement may be attributed to the contribution from incomplete fusion. The incomplete fusion strength function for ^{13}C+^{169}Tm is compared with that obtained in the ^{12}C+^{169}Tm system. It has been found that the one-neutron ($1n$) excess projectile ^{13}C (as compared to ^{12}C) results in a less incomplete fusion contribution due to its relatively large negative alpha-Q value. Recently proposed "alpha-Q-value systematics" seems to explain incomplete fusion data.

DOI: 10.1103/PhysRevC.89.024608 PACS number(s): 25.60.Dz, 25.70.Gh, 25.70.Jj

I. INTRODUCTION

The emission of fast projectile-like-fragments (PLF) in light heavy-ion (HI) interactions was first investigated by Britt and Quinton [1]. Similar observations were reported by Kauffman and Wolfgang [2], where fast PLF associated with massive transfer reactions were detected in the forward cone. The fast PLF production in massive transfer reactions was considered as a result of incomplete fusion (ICF) processes. In case of ICF, partial fusion of the projectile with the target nucleus takes place, leading to the formation of a "hot" metastable incompletely fused composite system with less mass, charge, and excitation energy as compared to the complete fusion (CF) population, where the entire projectile merges with the target nucleus [3,4]. Udagawa and Tamura [5,6] explained the production of PLF in massive transfer reactions (ICF) on the basis of the distorted-wave Born approximation (DWBA), in which the projectile is assumed to break up into constituent α clusters, e.g., ^{12}C may break up into ^{8}Be+α. One of the fragments may get fused with the target nucleus while the remnant behaves like a spectator dominantly emitted in the forward cone.

Widespread experimental and theoretical efforts have been devoted to understand the ICF dynamics [7–15], and several dynamical models have been proposed [5,6,16–24]. A description for the production of fast PLF was presented in Refs. [25,26]. The advances in the understanding of ICF dynamics took place after the particle-γ coincidence measurements by Inamura *et al.* [27] and Zolnowski *et al.* [28]. Apart from that, the correlation of energies and angles of charged particle(s) along with the γ multiplicity were measured by Geoffroy *et al.* [29], where the origin of PLF was investigated from undamped noncentral interactions. The noncentral nature of ICF was also emphasized by Trautmann *et al.* [30] and Inamura *et al.* [27,31]. In a review on ICF, Gerschel [32] inferred that the localization of the ℓ window also depends on the target deformation. For rare-earth targets, the emission of PLF was found to originate from high ℓ values [17,27,29,33], but the results obtained by Tricoire *et al.* [34] with semimagic targets suggested that the origin of direct PLF from the ℓ values is even smaller than $0.5\ell_{\rm crit}$ (where, "$\ell_{\rm crit}$" is the critical angular momentum) [35,36].

*phy.vijayraj@gmail.com
†bpsinghamu@gmail.com

Almost similar conclusions were drawn by Tserruya *et al.* [37] and Oeschler *et al.* [38], where both CF and ICF were observed below and above the value of ℓ_{crit}. Parker *et al.* [39], observed forward α particles in low-Z, HI interactions on a ^{51}V target at $\approx$ 6 MeV/A. The ICF systematics have also been explored for reactions with weakly bound projectiles, in studies investigating mechanisms of fusion suppression [40–43].

Some of the most widely employed models to explain ICF data are the (i) breakup fusion model [5,6,16], (ii) sum-rule model [17], (iii) exciton model [18], (iv) hot-spot [19], (v) promptly emitted particles model [20], and (vi) overlap model [21–24]. The aforementioned models have been used to fit the experimental data obtained at energies well above the Coulomb barrier (i.e., $E_{\text{lab}} \geqslant 10.5$ MeV/nucleon) but have shown certain failings in their ability to explain ICF data at relatively low bombarding energies (i.e., $\approx$ 3–7 MeV/nucleon) [44–51]. More recently, Diaz-Torres *et al.* [52] proposed a three-dimensional classical model for low-energy breakup fusion reactions. This model allows a consistent calculation of breakup, incomplete, and complete fusion cross-sections but is limited only for the weakly bound projectiles. Due to the unavailability of any reliable theoretical model to explain low-energy ICF data, the study of ICF is still an active area of investigations. Further, the observation of ICF at slightly above barrier energies where CF is supposed to be the sole contributor has triggered the study of low-energy ICF [3,44,45,53,54].

For the better understanding of ICF dynamics, the effect of various entrance channel parameters—namely, (a) projectile energy, (b) mass-asymmetry of interacting partners (μ_A), (c) α-Q value, and (d) input ℓ values—on the onset and strength of ICF need to be systematically investigated. In order to study low-energy ICF, several inclusive experiments have been performed at the Inter-University Accelerator Center (IUAC), New Delhi [44–48]. This work is an extension of our earlier measurements to study the effect of a one-neutron (1n) excess projectile on the onset and strength of ICF. In the present work, the excitation functions (EFs) of individual evaporation residues populated in ^{13}C and ^{169}Tm interactions have been measured at energies $\approx$ 4.4–6.5 MeV/nucleon. The experimental EFs have been analyzed in the framework of statistical model code PACE4 [55] to estimate the percentage fraction of ICF. The fraction of ICF obtained in the ^{13}C+^{169}Tm system has been compared with that obtained in the ^{12}C,^{16}O+^{169}Tm systems to display the behavior of ICF from non-α to α-cluster-structure projectiles. This paper is organized as follows. The experimental methodology and data reduction procedure are given is Sec. II, while Sec. III deals with the findings of the present work and discussion in connection with the existing results. The present work is summarized in Sec. IV of this paper.

II. EXPERIMENTAL PROCEDURE

The experiment was performed using ^{13}C^{6+} beam from the 15UD Pelletron accelerator at the IUAC, New Delhi. Self supporting ^{169}Tm targets of thickness $\approx$1.5–2.5 mg/cm^2, and Al-catcher foils of thickness $\approx$1.0–3.0 mg/cm^2 were prepared using a uniform pressure rolling technique. The thicknesses of each target and catcher foils were measured by the α-transmission method. The α-transmission method is based on the measurement of the energy lost by 5.487 MeV α particles emitted from a standard ^{241}Am source during the passage through the target and catcher foil.

Each target foil was backed by an Al-catcher foil of appropriate thickness to absorb the most energetic recoiling reaction products from the target foil. To cover a wide energy range in an irradiation, a stack of three target-catcher foil assemblies were irradiated in the general purpose scattering chamber (GPSC) at different energies, i.e., $E_{\text{lab}} \approx$ 65, 68, 82, 84, and 86 MeV. After the irradiations, the stack of target-catcher foil assemblies was taken out of the GPSC with the help of an in-vacuum transfer facility (ITF). A current integrator device installed at the beam dump was used to measure the beam current. A beam current of $\approx$2–3 p nA was maintained throughout the experiment. The activities produced after irradiations were recorded with a high-purity germanium (HPGe) detector of 100 cm^3 active volume coupled to a computer-automated measurement and control (CAMAC) based data acquisition system [56]. Several rounds of counting were initially performed for short durations (i.e., $\approx$15–30 seconds) to detect short-lived reaction residues, and then for long durations (i.e., $\approx$20–60 minutes) to detect relatively long-lived reaction residues. The HPGe detector was calibrated for both energy and efficiency using a ^{152}Eu source of known strength. The efficiency of the detector was determined for source-detector separations at which the counting of irradiated samples was done. The details of efficiency determination are given elsewhere [57]. The offline data analysis was performed using CANDLE software [56]. In the case of closely peaking doublets, the peak fitting was done both manually and by employing the auto-peak-search option. The width calibration was done using various standard γ sources, i.e., ^{60}Co, ^{133}Ba, ^{137}Cs, and ^{152}Eu.

A part of the γ-ray spectra obtained at $E_{\text{lab}} = 82.70 \pm 1.3$ MeV for the ^{13}C^{6+}+^{169}Tm system is shown in Fig. 1, where γ lines of different evaporation residues (ERs) are marked. The ERs have been identified by their characteristic γ lines and confirmed by their decay-curve analysis. As a representative

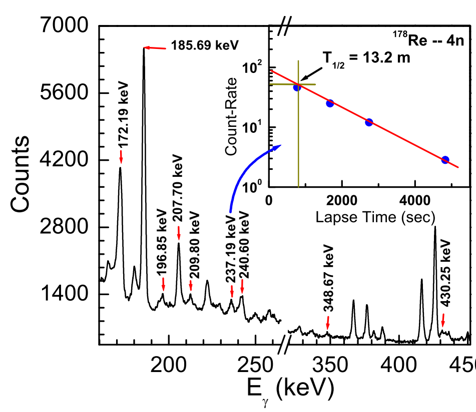

FIG. 1. (Color online) Typical gamma ray spectrum of ^{13}C+^{169}Tm interaction at 82.70 $\pm$ 1.3 MeV, where γ lines are assigned to different reaction products expected to be populated by CF and/or ICF.

TABLE I. Relevant nuclear data of the reaction residues identified in the present work.

Reactions	Residue	Half-life	J^π	E_γ (keV)	I_γ (%)	Mode
^{169}Tm(^{13}C,3n)	^{179}Re	19.7 min	3^+	430.25	28.0	$M1$
^{169}Tm(^{13}C,4n)	^{178}Re	13.2 min	$7/2^+$	106.06	23.1	$E2$
				237.19	45.0	$E2$
^{169}Tm(^{13}C,5n)	^{177}Re	14 min	$1/2^+$	196.85	100[a]	$E2$
				209.80	33.0[a]	$E2$
^{169}Tm(^{13}C,6n)	^{176}Re	5.2 min	$5/2^-$	108.9	100[a]	$E2$
				240.6	54[a]	$E2$
^{169}Tm(^{13}C,p4n)	^{177}W	132 min	$1/2^-$	115.05	59.0	$E1$
				185.69	16.1	$E1$
^{169}Tm(^{13}C,α3n)	^{175}Ta	10.5 h	$7/2^+$	207.70	13.3	$E1$
				348.67	11.4	$E2 + 47\%\ M1$
^{169}Tm(^{13}C,α4n)	^{174}Ta	1.18 h	3^+	206.38	57.7	$E2$
^{169}Tm(^{13}C,α5n)	^{173}Ta	3.65 h	$5/2^-$	172.19	17	$E2$
^{169}Tm(^{13}C,2α2n)	^{172}Lu	6.7 d	4^-	900.70	28.8	$M1$
				912.11	14.8	$M1 + E2$
				1093.67	63.5	$M1 + E2$
^{169}Tm(^{13}C,2α3n)	^{171}Lu	8.24 d	$7/2^+$	739.82	48.1	$E1$

[a]These intensities are relative.

case, a decay curve for ^{178}Re populated via the $4n$ channel is shown in the inset of Fig. 1. The measured half-lives of the ERs have been found to be in good agreement with the literature values [58]. The production cross sections of ERs have been calculated as described in Refs. [57,59,60]. The ERs identified in the present work are listed in Table I along with their spectroscopic properties [61]. The overall errors in the present measurement are estimated to be $\leqslant$10%. A detailed discussion on error analysis is presented in Refs. [57,62]. It may be pointed out that the possible effects from direct population of the ground states of ERs and transfer cross sections have not been considered due to their negligible contribution in the studied energy range and in the involved reaction channels. However, in Refs. [63,64], the ICF channels have been considered as transfer channels.

III. ANALYSIS OF EXPERIMENTAL DATA

The EFs of xn, pxn, αxn and $2\alpha xn$ channels expected to be populated via CF and/or ICF of ^{13}C with ^{169}Tm have been measured at energies $E_{\rm lab} \approx$ 59–85 MeV. The production possibilities of Re, W, Ta, and Lu isotopes via different reaction modes and decay routes are discussed in the following subsections. The higher charge isobar precursor contribution in the population of ^{177}W($p4n$) has been estimated from the cumulative cross section. The experimental EFs are analyzed within the framework of the statistical model code PACE4 [55]. In this code, the angular momentum conservation is explicitly taken into account and the CF cross-section is calculated using Bass's formula [65]. The partial cross section (σ_ℓ) for the formation of a compound nucleus (CN) at a particular angular momentum ℓ and at specific bombarding energy E is given by

$$\sigma_\ell = \frac{\lambda^2}{4\pi}(2\ell+1)T_\ell \tag{1}$$

where λ is reduced wavelength. The transmission coefficient T_ℓ may be given by the expression

$$T_\ell = \left[1+\exp\left(\frac{\ell-\ell_{\rm max}}{\Delta}\right)\right]^{-1} \tag{2}$$

where Δ is the diffuseness parameter, while $\ell_{\rm max}$ is the maximum amount of ℓ determined by the total fusion cross section

$$\sigma_F = \sum_{\ell=0}^{\infty}\sigma_\ell \tag{3}$$

The optical model potential of Becchetti and Greenlees [66] was used to calculate the transmission coefficients for neutron, proton, and α-particle emission. In the description of γ-ray competitions, the emissions of $E1$, $E2$, $M1$, and $M2$ γ rays are included and the γ-ray strength functions for different transitions are taken from the tables of Endt [67].

The nuclear level density ($a = A/K$) plays an important role in the fusion-evaporation component, where A is the atomic mass number and K is a parameter called the level density parameter. In order to choose the suitable value of level density to reproduce fusion EFs, different values of K = 8–12 have been tested and are plotted in Fig. 2(a). It may be pointed out that the code PACE4 predicts only CF channels, and does not take transfer and/or breakup ICF channels into account. Thus, a comparison of experimental EFs with the statistical model code PACE4 may indicate the extent to which the formation of identified ERs may be explained by the equilibrated CN decay. Any deviation in the experimental EFs with respect to the PACE4 predictions may be attributed to ICF, which is not included in this code [44–48].

A. EFs of *xn* and *pxn* channels

Figures 2(a) and 2(b) show the ratio of the individual cross sections for xn channels (σ_{xn}) to the sum of all measured xn

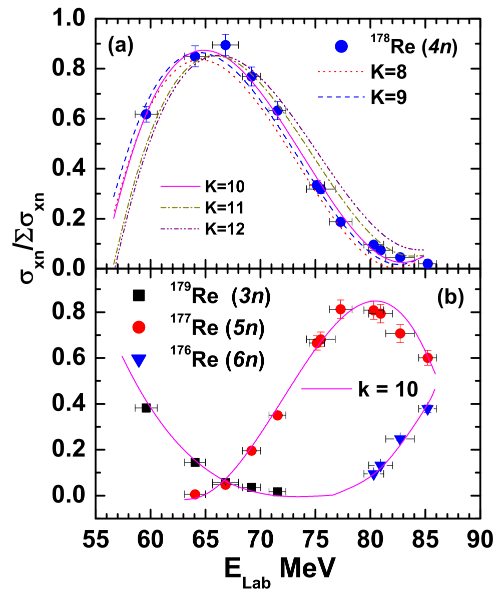

FIG. 2. (Color online) Ratio of individual channel cross section to the total channel cross section $\Sigma\sigma_{xn}$ as a function of laboratory energy for (a) measured $4n$ channel along with PACE4 predictions (for $K = 8$ to 12); (b) measured EFs for all xn ($x = 3$, 5, and 6) channels along with PACE4 calculations as discussed in the text.

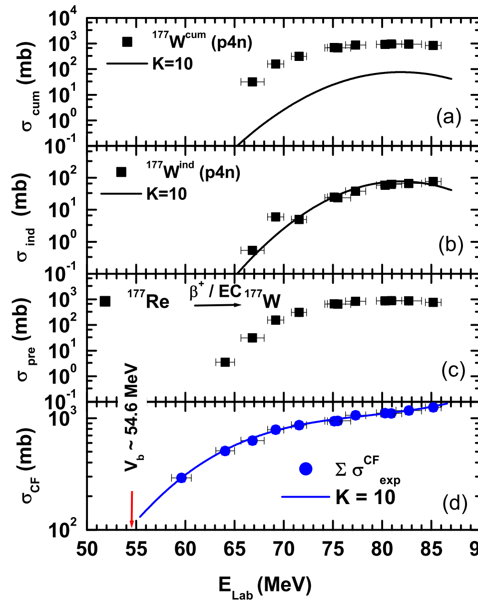

FIG. 3. (Color online) Experimentally measured EF of the ^{177}W ($p4n$) channel compared with PACE4 predictions: (a) cumulative cross section; (b) independent cross section. (c) Experimentally measured and theoretically predicted EFs of all xn and pxn channels compared. The solid lines are the PACE4 predictions at $K = 10$. In (d) V_b is the Coulomb barrier in laboratory frame.

channels. The above representation of experimental data has been chosen to observe the behavior of individual xn channels with respect to total fusion cross section. In Fig. 2(a), the PACE4 predictions for different level density parameters are shown for ^{178}Re residue populated via $4n$ channel. It is evident that the predictions of theoretical model code PACE4 with a value $K = 10$ satisfactorily reproduce the EFs of ^{178}Re evaporation residue. This suggests the population of ^{178}Re via emission of four neutrons from the excited ^{182}Re* formed via CF of ^{13}C with ^{169}Tm. As shown in Fig. 2(b), the same value of K fairly predicts the EFs for $3n$, $5n$, and $6n$ channels, indicating the involvement of the same mode of reaction.

Further, the experimental EFs for ^{177}W($p4n$) are compared with those predicted by the statistical model code PACE4 using the same set of input parameters in Fig. 3(a). As can be seen in this figure, PACE4 underpredicts the EFs for this residue. It may be pointed out that the β^+ decay from ^{177}Re nuclei may lead to ^{177}W. Therefore, ^{177}W may be populated independently via de excitation of ^{182}Re* compound nucleus by emitting a proton and four neutrons. Different possible decay routes to populate ^{177}W are

(i) $^{13}\text{C}+\,^{169}\text{Tm} \Rightarrow\, ^{182}\text{Re}^* \Rightarrow\, ^{177}\text{W} + p + 4n$,
(ii) $^{13}\text{C}+\,^{169}\text{Tm} \Rightarrow\, ^{182}\text{Re}^* \Rightarrow\, ^{177}\text{Re} + 5n$,
i.e., $^{177}\text{Re} \xrightarrow{\beta^+/EC}\, ^{177}\text{W}$.

As proposed by Cavinato *et al.* [68], the independent cross-section (σ_{ind}) of ^{177}W has been estimated from the cumulative cross section (σ_{cum}) as

$$\sigma_{\text{ind}} = \sigma_{\text{cum}} - P_{\text{pre}}\frac{t^d_{1/2}}{\left(t^d_{1/2} - t^{\text{pre}}_{1/2}\right)}\sigma_{\text{pre}}, \tag{4}$$

where σ_{pre} is the cross section of the parent nuclei, $t^d_{1/2}$ and $t^{\text{pre}}_{1/2}$ are the half-lives of daughter and precursor nuclei. The P_{pre} is the branching ratio of the precursor to its daughter nuclei. The above formulation to calculate independent yield is obtained for $t^d_{1/2} > t^{\text{pre}}_{1/2}$; i.e., $t^d_{1/2} \approx 132$ min for $^{177}\text{W} > t^{\text{pre}}_{1/2} \approx 14$ min for ^{177}Re. The σ_{ind} of ^{177}W can be calculated as

$$\sigma_{\text{ind}}(^{177}\text{W}) = \sigma_{\text{cum}}(^{177}\text{W}) - 1.118\sigma_{\text{pre}}(^{177}\text{Re}). \tag{5}$$

The σ_{ind} of ^{177}W is compared with PACE4 predictions in Fig. 3(b). As shown in this figure, the EF of ^{177}W shows good agreement with PACE4 predictions, which suggests the population of this nuclei via CF. The precursor decay contributions are also plotted separately in Fig.3(c) to show that due to the short half-life of the precursor it decays rapidly via β^+/EC giving a substantial contribution to the cumulative cross section of ^{177}W. In Fig. 3(d), the sum of all CF channels ($\Sigma\sigma^{\text{exp}}_{\text{CF}}$) is compared with PACE4 predictions (i.e., $\Sigma\sigma^{th}_{\text{CF}}$). The values of $\Sigma\sigma^{\text{exp}}_{\text{CF}}$ at different energies are found to be in good agreement with those predicted by PACE4. This gives confidence in the choice of input parameters of the theoretical model code. Therefore, the same set of input parameters can be used to fit the EFs of all α-emitting channels.

B. EFs of α-emitting channels

Reaction residues ^{173,174,175}Ta and ^{171,172}Lu are populated via emission of $\alpha3n$, $\alpha4n$, $\alpha5n$, $2\alpha2n$, and $2\alpha3n$ respectively. These residues are expected to be populated via both CF and/or ICF. It is relevant to mention that ICF is not taken into consideration in PACE4; therefore, calculation of cross sections for α-emitting channels with this code may illuminate the underlying physical effects. The experimental EFs of individual α-emitting channels are compared with PACE4

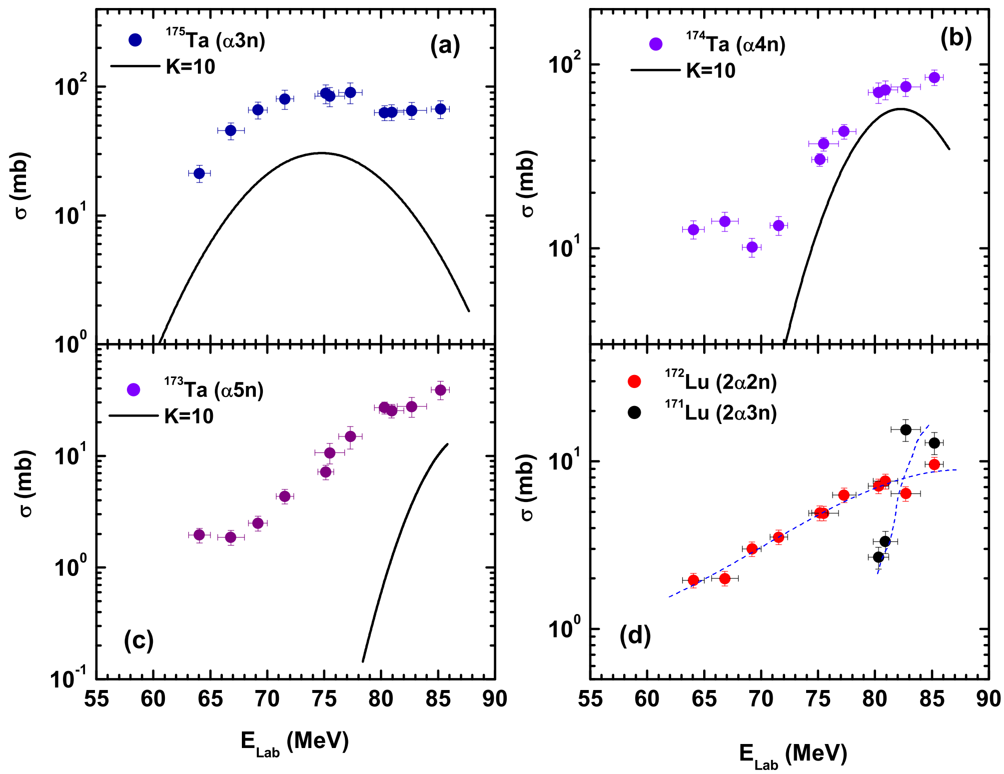

FIG. 4. (Color online) Experimentally measured EFs of ERs ^{175}Ta, ^{174}Ta, ^{173}Ta, ^{172}Lu, and ^{171}Lu are compared with the PACE4 predictions. Solid black curves represent theoretical calculations as described in the text. In panel (d) the dotted lines through the data points are drawn to show the trend of the excitation function.

predictions in Figs. 4(a)–4(d). As shown in Figs. 4(a)–4(c), the experimental EFs of ^{173,174,175}Ta residues are significantly enhanced as compared to the PACE4 predictions for the studied energy range. The enhancement in experimental EFs over PACE4 predictions may be attributed to the ICF processes. For example, the evaporation residue ^{174}Ta may be populated via both CF and/or ICF through three routes:

(i) CF → decay of ^{182}Re* via two protons and six neutrons ($2p6n$ channel),

$$^{13}\text{C}+{}^{169}\text{Tm} \Rightarrow {}^{182}\text{Re}^* \Rightarrow {}^{174}\text{Ta} + 2p6n,$$
$$Q \text{ value} \approx -69.15 \text{ MeV},$$
$$E_{Th} \approx 74.47 \text{ MeV}.$$

(ii) CF → decay of ^{182}Re* via an α particle and four neutrons ($\alpha 4n$ channel),

$$^{13}\text{C} + {}^{169}\text{Tm} \Rightarrow {}^{182}\text{Re}^* \Rightarrow {}^{174}\text{Ta} + \alpha 4n,$$
$$Q \text{ value} \approx -40.86 \text{ MeV},$$
$$E_{Th} \approx 43.99 \text{ MeV}.$$

(iii) ICF → breakup of ^{13}C (i.e., ^{9}Be + α), where ^{9}Be fuses with ^{169}Tm forming a ^{178}Ta* composite system and an α particle moves in the forward direction as a spectator. The reduced excited compound nucleus ^{178}Ta* decays through the emission of 4 neutrons,

$$^{13}\text{C}(^{9}\text{Be} + \alpha) \Rightarrow {}^{9}\text{Be} + {}^{169}\text{Tm} \Rightarrow {}^{178}\text{Ta}^*$$

(α as a spectator)

$$\Rightarrow {}^{178}\text{Ta}^* \Rightarrow {}^{174}\text{Ta} + 4n,$$
$$Q \text{ value} \approx -30.21 \text{ MeV},$$
$$E_{Th} \approx 31.82 \text{ MeV}.$$

Figure 4(d) shows EFs for ^{171,172}Lu residues where the statistical model code PACE4 predicts negligible cross section, indicating their population solely via ICF processes. As such, it can be inferred that the ICF significantly contributes in the production of ^{173,174,175}Ta and ^{171,172}Lu isotopes. In order to account for the ICF fraction in the studied α-emitting channels, the sum of all α-emitting channels ($\Sigma\sigma_{\text{exp}}^{\alpha' s}$) is compared with that predicted by PACE4 ($\Sigma\sigma_{\text{PACE4}}^{\alpha' s}$) in Fig. 5(a). The ICF fraction at different energies is calculated as $\sigma_{\text{ICF}} = \Sigma\sigma_{\text{exp}}^{\alpha' s} - \Sigma\sigma_{\text{PACE4}}^{\alpha' s}$ [69,70]. For better visualization of increasing ICF contribution with incident projectile energy, the value of $\Sigma\sigma_{\text{ICF}}$ is plotted in Fig. 5(b), which reflects strong energy dependence of the ICF fraction. It may not be out of place to mention that the contribution shown in Fig. 5(b) gives the lower limit of ICF because all the expected α-emitting channels could not be measured.

C. Onset and strength of ICF

For better insight into the onset and strength of ICF, the ICF strength function (F_{ICF}) has been derived from the analysis of experimental EFs in the ^{13}C+^{169}Tm system which defines empirical probability of ICF at different projectile energies, and is plotted in Fig. 6(a). As shown in this figure, the value of F_{ICF} linearly increases from ≈5% (at ≈16% above the barrier) to ≈10% (at ≈56% above the barrier). This suggests strong projectile energy dependence of ICF reactions. The present results are found to be qualitatively consistent with

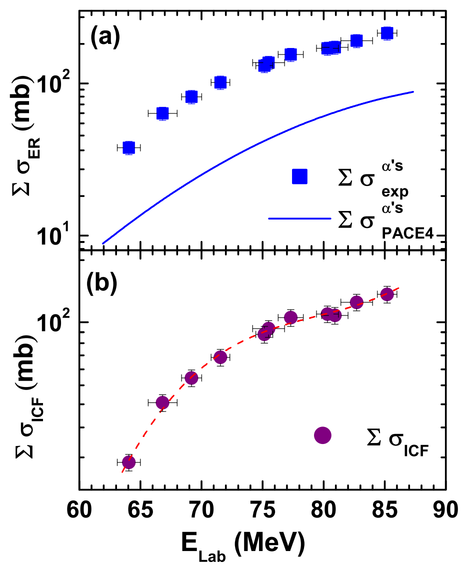

FIG. 5. (Color online) (a) Sums of all experimentally measured cross sections for α and 2α emitting channels are compared with correcting PACE4 prediction. The values of $\Sigma\sigma_{\text{exp}}^{\alpha's}$ are significantly higher than that predicted by PACE4. (b) Deduced σ_{ICF} is plotted as a function of beam energy. The dashed line through the data points in (b) is drawn just to guide the eyes.

that presented for the ^{12}C+^{169}Tm system by Singh *et al.* [54]. In Fig. 6(b), the values of F_{ICF} obtained in the ^{13}C+^{169}Tm system (present work) are compared with those obtained in the ^{12}C+^{169}Tm system [54] as a function of v_{rel} to probe the effect of one-neutron (1n) excess projectile on the onset and strength of ICF. According to Morgenstern's systematics [71,72], ICF contributes significantly above $v_{\text{rel}} \approx 0.06$ (6% of c). As shown in Fig. 6(b), the values of v_{rel} are in the range from $\approx$0.04 (4% of c) to $\approx$0.07 (7% of c) for the ^{13}C projectile. The results presented in Fig. 6(b) clearly demonstrate the onset of ICF at the relatively lower value of v_{rel}, i.e., $\approx$0.04 ($F_{\text{ICF}} \approx 4\%$) in the ^{13}C+^{169}Tm system. In this case, the observed value of F_{ICF} is significant at well below the proposed onset value of v_{rel} (i.e., 6% of c). As such, it can be inferred that the ICF starts competing with CF even at slightly above barrier energies.

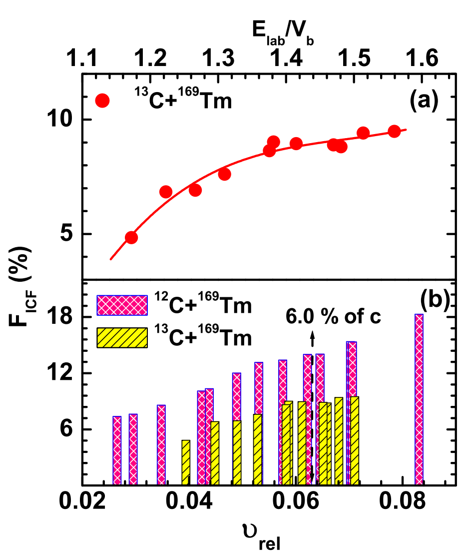

FIG. 6. (Color online) (a) Deduced F_{ICF}as a function of normalized energy and (b) a comparison of deduced F_{ICF} as a function of relative velocity (v_{rel}/c) for ^{13,12}C+^{169}Tm systems, respectively. In (a), the line is drawn to guide the eyes.

Further, as shown in Fig. 6(b), the values of F_{ICF} for the ^{13}C projectile are less than for the ^{12}C projectile in the studied energy range. The difference in F_{ICF} for two systems (^{13}C,^{12}C+^{169}Tm) is clearly evident, which indicates the strong projectile dependence of F_{ICF}. It may be pointed out that the ^{12}C projectile is an α-cluster nuclei, which may break up into several combinations of α clusters. Some of the breakup combinations which have been observed in previous studies are ^{12}C $\rightarrow$ ^{8}Be+^{4}He(α) and/or three α fragments. One or a group of fragments may fuse with the target nucleus to form an incompletely fused composite system. In the case of the ^{13}C projectile, one-neutron (1n) excess modifies the breakup probability, which may eventually affect the fraction of ICF. The ^{12}C projectile may open up more ICF channels as compared to the ^{13}C induced reactions.

D. Projectile structure dependence of ICF

As discussed in the previous section, onset and fraction of ICF are found to be noticeably different for ^{13}C+^{169}Tm and ^{12}C+^{169}Tm systems, which may be the effect of an additional neutron as compared to the ^{12}C projectile. In order to better understand the projectile structure dependence of ICF, the radii of ^{13}C and ^{12}C have been calculated using the standard formula i.e., $R = R_0 A^{1/3}$ (keeping $R_0 = 1.2$ fm), and have been found to be $\approx$2.821 and $\approx$2.747 fm for ^{13}C and ^{12}C, respectively. It may be pointed out that no physically reasonable relationship of ICF fraction with the projectile size could be obtained. The differences in the values of ICF fraction at the same normalized energies for two projectile-target combinations may be due to the projectile structure effects. In this regard, the projectile binding energy may play an important role. The binding energy per nucleon (E_B/A) for ^{13}C and ^{12}C projectiles are found to be 7.469 and 7.680 MeV, respectively.

The fact that the ^{12}C is more strongly bound than the ^{13}C projectile suggests a larger breakup probability for ^{13}C projectile. However, in the present case contradictory results in terms of binding energy have been observed. Similar observations have been made in the cases of ^{12}C,^{13}C+^{159}Tb [44,53] and ^{12}C,^{13}C+^{181}Ta [49] systems. In order to explore this issue, the ICF strength functions in ^{12}C,^{13}C+^{169}Tm systems have been studied in terms of projectile α-Q value in which the projectiles may be assumed to break up into the following channels:

$$^{12}C \Rightarrow {}^{8}\text{Be} + \alpha,\ Q_\alpha = -7.37\ \text{MeV},$$
$$^{13}C \Rightarrow {}^{9}\text{Be} + \alpha,\ Q_\alpha = -10.64\ \text{MeV}.$$

As indicated above, the α-Q value (Q_α) for the non-α-cluster (^{13}C) projectile is more negative than that of the α-cluster (^{12}C) projectile. This translates into less fusion incompleteness for a one-neutron (1n) excess projectile than that observed for the ^{12}C projectile.

TABLE II. Experimentally measured production cross sections for the residues populated via CF only.

E_{Lab} (MeV)	^{179}Re	^{178}Re	^{177}Re	^{176}Re	^{177}W
59.60 ± 1.0	125.14 ± 18.77	202.44 ± 31.86			
64.05 ± 0.95	80.21 ± 15.5	473.61 ± 76.04	3.21 ± 0.51		
66.82 ± 1.18	33.45 ± 5.01	530.12 ± 73.80	28.40 ± 9.64		0.53 ± 0.09
69.18 ± 0.8	25.65 ± 3.8	552.13 ± 82.81	140.25 ± 24.03		6.23 ± 1.08
71.55 ± 0.77	13.63 ± 2.04	506.76 ± 91.01	280.51 ± 35.38		5.09 ± 0.9
75.14 ± 0.7		303.13 ± 47.05	603.10 ± 84.2		25.52 ± 4.5
75.49 ± 1.31		280.67 ± 45.18	600.23 ± 87		23.60 ± 4.23
77.30 ± 1.02		176.95 ± 26.5	765.49 ± 122.47		38.22 ± 6.84
80.31 ± 0.9		94.20 ± 16.24	790.80 ± 111.7	92.87 ± 14.85	59.10 ± 10.63
80.92 ± 1.08		75.93 ± 9.43	810.67 ± 121.3	135.33 ± 21.65	62.32 ± 11.21
82.7 ± 1.3		52.16 ± 7.81	800.26 ± 135.88	279.75 ± 28.76	66.34 ± 11.88
85.2 ± 0.8		23.50 ± 3.52	695.98 ± 111.1	438.62 ± 54.1	76.42 ± 13.75

Further, the values of F_{ICF} have been plotted as a function of Q_α at different relative velocities in Figs. 7(a)–7(c). The value of F_{ICF} for the ^{16}O projectile ($Q_\alpha \approx -7.16$ MeV) is also compared in this figure. As shown in this figure, the values of F_{ICF} fall off systematically for more negative Q_α projectiles (i.e., ^{16}O, ^{12}C, and ^{13}C). Therefore, it can be safely inferred that the Q_α is a rather more suitable parameter than binding energy to explain ICF data. In order to strengthen the above systematics, the values of F_{ICF} for ^{12}C,^{13}C,^{16}O+^{159}Tb [44,53,73] and ^{12}C,^{13}C,^{16}O+^{181}Ta [46,49] systems have been compared in Figs. 8(a) and 8(b) as a functions of Q_α at the same value of of v_{rel}. As indicated in this figure, the probability of ICF is found to be higher for less negative Q_α projectiles. The present results are in good agreement with that presented in Ref. [49,53].

E. Target dependence of ICF

In earlier sections, it has been demonstrated that the onset and strength of ICF strongly depend on projectile energy, structure, and Q_α. It may be interesting to extend this study to the target dependence on ICF fraction. In order to display target dependence, the value of the ICF fraction for the ^{13}C+^{169}Tm system (present work) is plotted with that obtained in the ^{13}C+^{159}Tb [53] and ^{13}C+^{181}Ta [49] systems as a function of mass asymmetry (μ_A) for a constant relative velocity (i.e., $v_{rel} \approx 0.053c$) in Fig. 9. As indicated in this figure, the values of F_{ICF} are found to be more for more mass-asymmetric systems. The present results are in agreement with mass-asymmetry systematics proposed by Morgenstern *et al*. [63,71,72]. It may be pointed out that the values of F_{ICF} for the ^{13}C+^{181}Ta system are off from the increasing trend shown with a straight line. It may be because of the fact that several expected α-emitting channels could not be measured or observed due to their short half-lives and/or very low intensities in this work.

F. Fusion ℓ distribution

In HI reactions, input angular momentum ℓ is a sensitive entrance channel parameter which has been reported to be responsible for the low-energy CF. In order to study ℓ distribution for presently studied system, the values of maximum angular momentum (ℓ_{max}) and critical angular momentum for fusion to occur (ℓ_{crit}) in the ^{12}C,^{13}C+^{169}Tm systems are calculated. The ℓ_{max} is defined as the largest ℓ for which the colliding system penetrates into the region where the total nucleus-nucleus potential is attractive and/or the distance of closest approach is smaller than the sum of the half-density radii. However, the ℓ_{crit} is the limiting angular momentum for fusion to occur, which determines the magnitude of the transmission coefficients T_ℓ for individual reaction channels, and may be calculated from

TABLE III. Experimentally measured production cross sections of the residues populated via CF and/or ICF.

E_{Lab} (MeV)	^{175}Ta	^{174}Ta	^{173}Ta	^{172}Lu	^{171}Lu
64.05 ± 0.95	21.22 ± 3.19	12.65 ± 1.39	1.95 ± 0.29	1.95 ± 0.21	
66.82 ± 1.18	45.61 ± 6.84	14.01 ± 1.54	1.86 ± 0.27	2.01 ± 0.22	
69.18 ± 0.8	65.98 ± 9.75	10.11 ± 1.11	2.54 ± 0.37	3.22 ± 0.33	
71.55 ± 0.77	80.32 ± 13.6	13.28 ± 1.46	4.35 ± 0.65	3.53 ± 0.38	
75.14 ± 0.7	88.35 ± 14.75	30.27 ± 3.34	7.16 ± 1.07	4.91 ± 0.55	
75.49 ± 1.31	84.35 ± 14.12	36.95 ± 4.01	10.69 ± 2.20	4.91 ± 0.53	
77.30 ± 1.02	90.12 ± 16.61	43.19 ± 4.7	14.91 ± 3.4	6.30 ± 0.69	
80.31 ± 0.9	62.92 ± 8.38	70.32 ± 7.73	26.92 ± 3.2	7.12 ± 0.78	2.67 ± 0.41
80.92 ± 1.08	63.41 ± 9.061	72.77 ± 8.00	25.40 ± 3.51	7.59 ± 0.83	3.31 ± 0.49
82.7 ± 1.3	65.56 ± 9.75	75.46 ± 8.30	27.77 ± 5.56	6.41 ± 0.70	15.44 ± 2.31
85.2 ± 0.8	67.17 ± 10.67	85.12 ± 9.36	39.04 ± 7.35	9.61 ± 1.05	12.88 ± 1.93

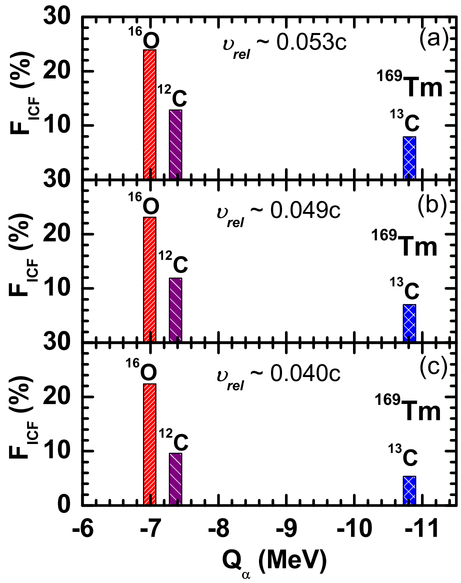

FIG. 7. (Color online) Comparison of $F_{\rm ICF}$ on the basis of α-Q values at three different constant relative velocities [$\nu_{\rm rel} \approx$ (a) 0.053c, (b) 0.049c, and (c) 0.040c]. For ^{13,12}C+^{169}Tm systems, data is taken from Refs. [45,54].

a simplified formula [74] as

$$\ell_{\rm crit}^2 = \frac{\mu_m (C_1 + C_2)^3}{\hbar^2}\left[4\pi\gamma\frac{C_1 C_2}{C_1 + C_2} - \frac{Z_1 Z_2 e^2}{(C_1 + C_2)^2}\right], \quad (6)$$

where μ_m is the reduced mass of the interacting partners, γ is the surface tension coefficient, Z_1, Z_2 and C_1, C_2 are the atomic numbers and half-density radii of projectile and target nuclei, respectively. From the above equation, the calculated values of $\ell_{\rm crit}$ for the ^{12}C,^{13}C+^{169}Tm systems turn out to be

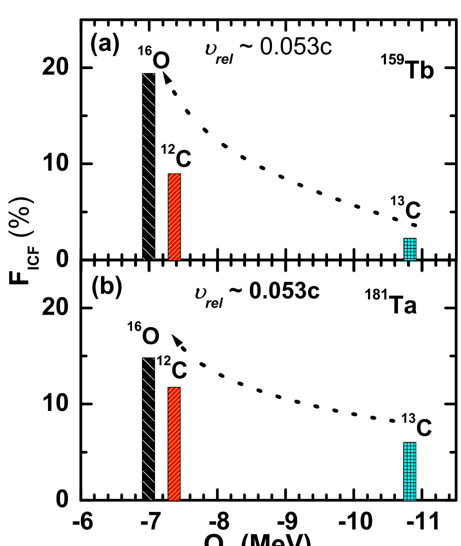

FIG. 8. (Color online) Comparison of $F_{\rm ICF}$ on the basis of α-Q value of the projectile at a constant $\nu_{\rm rel} = 0.053c$ for different projectile-target combinations (^{12,13}C+^{159}Tb [44,53], ^{16}O+^{159}Tb [73], ^{16}O+^{181}Ta [46], and ^{12,13}C+^{181}Ta [49]). For details see text.

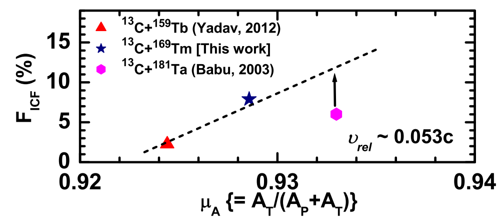

FIG. 9. (Color online) Deduced percentage ICF fraction ($F_{\rm ICF}$) for the present system (^{13}C+^{169}Tm) as a function of mass symmetry at $\nu_{\rm rel} \approx 0.053c$ along with values available in literature (^{13}C+^{159}Tb [53], ^{13}C+^{181}Ta [49]). The solid line is drawn to guide the eyes.

$\approx 52\hbar$ and $\approx 48\hbar$, respectively. The values of the $\ell_{\rm max}$ have been calculated using the code CCFULL [75] with Woods-Saxon potential depth $V_0 \approx 105$ MeV and the radius parameter $R_0 \approx 1.1$ fm. In the present work, no coupling condition is used in $\ell_{\rm max}$ calculations. Because the strongly bound projectiles have relatively high breakup thresholds, coupling to the breakup channels plays a small role in fusion reactions.

The fusion ℓ distribution has been calculated for three values of A_0 (i.e., $\approx$0.50, 0.70, and 0.90 fm) and are plotted in Figs. 10(a)–10(c) at the highest studied energy to display the effect of surface diffuseness parameter A_0 on $\ell_{\rm max}$. As shown in Figs. 10(a)–10(c), the lower value of diffuseness parameter

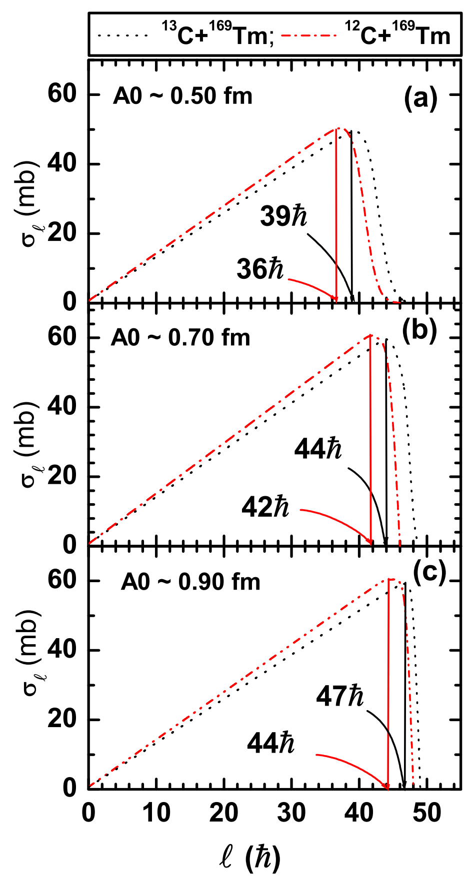

FIG. 10. (Color online) Fusion ℓ distributions calculated using code CCFULL [75] for ^{13}C+^{169}Tm and ^{12}C+^{169}Tm [54] systems at 85.2 MeV projectile energy for three different diffuseness parameter A_0, i.e., (a) 0.50, (b) 0.70, and (c) 0.90.

decreases the value of ℓ_{max}, which results in the reduction of the fusion cross section. The values of ℓ_{max} for the ^{12}C,$^{13}C+^{169}Tm$ systems calculated at ≈85 MeV for $A_0 \approx 0.70$ fm are found to be ≈44$\hbar$ and ≈42$\hbar$, respectively. For $A_0 \approx 0.90$ fm, the values of ℓ_{max} increas by ≈3$\hbar$ for the $^{13}C+^{169}Tm$ system and ≈2$\hbar$ for the $^{12}C+^{169}Tm$ system. In the present work, the values of ℓ_{max} are smaller than the values of ℓ_{crit}, indicating no fusion above ℓ_{crit}, which suggests that the partial waves below ℓ_{crit} also contribute to the ICF processes [51,76].

IV. SUMMARY AND CONCLUSIONS

In the present work, the EFs for several evaporation residues populated via CF and/or ICF of ^{13}C with ^{169}Tm have been measured at energies ≈4.4–6.5 MeV/nucleon and analyzed in the framework of statistical model code PACE4. Experimentally measured EFs of xn/pxn channels have been well reproduced with PACE4 predictions, indicating the population of these channels solely via CF. However, in the case of all α-emitting channels, experimental EFs have been found to be significantly enhanced as compared to the predictions of PACE4. This enhancement has been assumed to be attributed to the onset of ICF. The value of the independent production cross section for the $p4n$ channel has been deduced from the cumulative and precursor decay contributions due to its higher charge isobar.

A systematic analysis of ICF dependence on various entrance channel parameters has been performed. It has been found that ICF strongly depends on incident energy, projectile and target type, α-Q value,and ℓ values. Results and analysis presented on projectile structure effects suggest more ICF fraction for less negative α-Q value projectiles. Results presented in this paper are in good agreement with the existing data [53]. Further, the measurement of forward ranges and spin distributions of reactions recoils may provide a more clear and conclusive picture of the incomplete fusion processes.

ACKNOWLEDGMENTS

The authors thank the Director of IUAC, New Delhi and the Chairman of the Department of Physics, Aligarh Muslim University for providing all the necessary facilities to carry out this work. R.P., B.P.S., and V.R.S. thank the UGC for Project No. 40-418/2011 (SR), and to DST for financial support. One of the authors (D.P.S.) thanks DST for providing YS fellowship under Project No. SR/FTP/PS-025/2011. One of the authors V.R.S. thankful to Prof. R. K. Bhowmik, IUAC for their valuable suggestions on ICF.

[1] H. C. Britt and A. R. Quinton, Phys. Rev. **124**, 877 (1961).
[2] R. Kauffmann and R. Wolfgang, Phys. Rev. **121**, 206 (1961).
[3] P. P. Singh *et al.*, Phys. Lett. B **671**, 20 (2009), and references therein.
[4] G. J. Lane, G. D. Dracoulis, A. P. Byrne, A. R. Poletti, and T. R. McGoram, Phys. Rev. C **60**, 067301 (1999), and references therein.
[5] T. Udagawa and T. Tamura, Phys. Rev. Lett. **45**, 1311 (1980).
[6] T. Udagawa and T. Tamura, Phys. Lett. B **116**, 311 (1982).
[7] M. S. Hussein, M. P. Pato, L. F. Canto, and R. Donangelo, Phys. Rev. C **46**, 377 (1992); Nucl. Phys. A **588**, 85c (1995); M. S. Hussein and A. F. R. de Toledo Piza, Phys. Rev. Lett. **72**, 2693 (1994).
[8] K. Yabana, Prog. Theor. Phys. **97**, 437 (1997).
[9] A. Diaz-Torres and I. J. Thompson, Phys. Rev. C **65**, 024606 (2002).
[10] K. Hagino, A. Vitturi, C. H. Dasso, and S. M. Lenzi, Phys. Rev. C **61**, 037602 (2000).
[11] A. Yoshida, C. Signorini, T. Fukuda, Y. Watanabe, N. Aoi, M. Hirai, M. Ishihara, H. Kobinata, Y. Mizoi, L. Mueller, Y. Nagashima, J. Nakano, T. Nomura, Y. H. Pu, and F. Scarlassara, Phys. Lett. B **389**, 457 (1996).
[12] J. J. Kolata, V. Guimarães, D. Peterson, P. Santi, R. White-Stevens, P. A. DeYoung, G. F. Peaslee, B. Hughey, B. Atalla, M. Kern, P. L. Jolivette, J. A. Zimmerman, M. Y. Lee, F. D. Becchetti, E. F. Aguilera, E. Martinez-Quiroz, and J. D. Hinnefeld, Phys. Rev. Lett. **81**, 4580 (1998).
[13] K. E. Rehm, H. Esbensen, C. L. Jiang, B. B. Back, F. Borasi, B. Harss, R. V. F. Janssens, V. Nanal, J. Nolen, R. C. Pardo, M. Paul, P. Reiter, R. E. Segel, A. Sonzogni, J. Uusitalo, and A. H. Wuosmaa, Phys. Rev. Lett. **81**, 3341 (1998).
[14] M. Dasgupta, D. J. Hinde, R. D. Butt, R. M. Anjos, A. C. Berriman, N. Carlin, P. R. S. Gomes, C. R. Morton, J. O. Newton, A. Szanto de Toledo, and K. Hagino, Phys. Rev. Lett. **82**, 1395 (1999).
[15] M. Dasgupta, D. J. Hinde, K. Hagino, S. B. Moraes, P. R. S. Gomes, R. M. Anjos, R. D. Butt, A. C. Berriman, N. Carlin, C. R. Morton, J. O. Newton, and A. Szanto de Toledo, Phys. Rev. C **66**, 041602(R) (2002).
[16] E. Takada, T. Shimoda, N. Takahashi, T. Yamaya, K. Nagatani, T. Udagawa, and T. Tamura, Phys. Rev. C **23**, 772 (1981).
[17] J. Wilczynski, K. Siwek-Wilczynska, J. Van Driel, S. Gonggrijp, D. C. J. M. Hageman, R. V. F. Janssens, J. Lukasiak, R. H. Siemssen, and S. Y. Van Der Werf, Nucl. Phys. A **373**, 109 (1982).
[18] M. Blann, Phys. Lett. **27**, 337 (1971).
[19] R. Weiner and Westrom, Nucl. Phys. A **286**, 282 (1977).
[20] J. P. Bondrof *et al.*, Nucl. Phys. A **333**, 285 (1980).
[21] B. G. Harvey, Phys. Lett. B **130**, 373 (1983).
[22] B. G. Harvey, Nucl. Phys. A **444**, 498 (1985).
[23] A. Y. Abul-Magd, Z. Phys. A **298**, 143 (1980).
[24] M. H. Simbel and A. Y. Abul-Magd, Z. Phys. A **294**, 277 (1980).
[25] C. K. Gelbke, D. K. Scott, M. Bini, D. L. Hendrie, J. L. Laville, J. Mahoney, M. C. Mermaz, and C. Olmer, Phys. Lett. B **70**, 415 (1977).
[26] J. B. Ball, C. B. Fulmer, M. L. Mallory, and R. L. Robinson, Phys. Rev. Lett. **40**, 1698 (1978).
[27] T. Inamura, M. Ishihara, T. Fukuda, T. Shimoda, and H. Hiruta, Phys. Lett. B **68**, 51 (1977); T. Inamura, A. C. Kahler, D. R. Zolnowski, U. Garg, T. T. Sugihara, and M. Wakai, Phys. Rev. C **32**, 1539 (1985).
[28] D. R. Zolnowski, H. Yamada, S. E. Cala, A. C. Kahler, and T. T. Sugihara, Phys. Rev. Lett. **41**, 92 (1978).
[29] K. A. Geoffroy, D. G. Sarantites, M. L. Halbert, D. C. Hensley, R. A. Dayras, and J. H. Barker, Phys. Rev. Lett. **43**, 1303 (1979).

[30] W. Trautmann, Ole Hansen, H. Tricoire, W. Hering, R. Ritzka, and W. Trombik, Phys. Rev. Lett. **53**, 1630 (1984).
[31] T. Inamura, T. Kojima, T. Nomura, T. Sugitate, and H. Utsunomiya, Phys. Lett. B **84**, 71 (1979).
[32] C. Gerschel, Nucl. Phys. A **387**, 297 (1982).
[33] J. H. Barker, J. R. Beene, M. L. Halbert, D. C. Hensley, M. Jaaskelainen, D. G. Sarantites, and R. Woodward, Phys. Rev. Lett. **45**, 424 (1980).
[34] H. Tricoire, C. Gerschel, A. Gillibert, and N. Perrin, Z. Phys. A **323**, 163 (1986).
[35] R. L. Robinson *et al.*, Phys. Rev. C **24**, 2084 (1981).
[36] H. Utsunomiya, T. Nomura, M. Ishihara, T. Sugitate, K. Ieki, and S. Kohmoto, Phys. Lett. B **105**, 135 (1981).
[37] I. Tserruya, V. Steiner, Z. Fraenkel, P. Jacobs, D. G. Kovar, W. Henning, M. F. Vineyard, and B. G. Glagola, Phys. Rev. Lett. **60**, 14 (1988).
[38] H. Oeschler, M. Kollatz, W. Bohne, K. Grabisch, H. Lehr, H. Freiesleben, and K. D. Hildenbrand, Phys. Lett. B **127**, 177 (1983).
[39] D. J. Parker, J. J. Hogan, and J. Asher, Phys. Rev. C **39**, 2256 (1989).
[40] P. R. S. Gomes, R. Linares, J. Lubian, C. C. Lopes, E. N. Cardozo, B. H. F. Pereira, and I. Padron, Phys. Rev. C **84**, 014615 (2011).
[41] R. Rafiei, R. duRietz, D. H. Luong, D. J. Hinde, M. Dasgupta, M. Evers, and A. Diaz-Torres, Phys. Rev. C **81**, 024601 (2010).
[42] D. J. Hinde, M. Dasgupta, B. R. Fulton, C. R. Morton, R. J. Wooliscroft, A. C. Berriman, and K. Hagino, Phys. Rev. Lett. **89**, 272701 (2002).
[43] P. R. S. Gomes *et al.*, Phys. Rev. C **73**, 064606 (2006); Phys. Lett. B **601**, 20 (2004).
[44] A. Yadav, V. R. Sharma, P. P. Singh, D. P. Singh, M. K. Sharma, U. Gupta, R. Kumar, B. P. Singh, R. Prasad, and R. K. Bhowmik, Phys. Rev. C **85**, 034614 (2012).
[45] P. P. Singh, B. P. Singh, M. K. Sharma, Unnati, D. P. Singh, and R. Prasad, Phys. Rev. C **77**, 014607 (2008).
[46] D. P. Singh, Unnati, P. P. Singh, A. Yadav, M. K. Sharma, B. P. Singh, K. S. Golda, R. Kumar, A. K. Sinha, and R. Prasad, Phys. Rev. C **80**, 014601 (2009).
[47] A. Yadav *et al.*, International Conference on Frontiers in Gamma Spectroscopy, 2012 (private communication).
[48] M. K. Sharma, Unnati, D. P. Singh, P. P. Singh, B. P. Singh, R. Prasad, and H. D. Bhardwaj, Phys. Rev. C **75**, 064608 (2007).
[49] K. Surendra Babu, R. Tripathi, K. Sudarshan, B. D. Shrivastava, A. Goswami, and B. S. Tomar, J. Phys. G **29**, 1011 (2003).
[50] K. Sudarsan Babu *et al.*, Nucl. Phys. A **739**, 229 (2004).
[51] R. Tripathi, K. Sudarshan, S. Sodaye, S. K. Sharma, A. V. R. Reddy, and A. Goswami, Eur. Phys. J. A **42**, 25 (2009).
[52] A. Diaz-Torres, D. J. Hinde, J. A. Tostevin, M. Dasgupta, and L. R. Gasques, Phys. Rev. Lett. **98**, 152701 (2007).
[53] A. Yadav, V. R. Sharma, P. P. Singh, R. Kumar, D. P. Singh, Unnati, M. K. Sharma, B. P. Singh, and R. Prasad, Phys. Rev. C **86**, 014603 (2012), and references therein.
[54] P. P. Singh *et al.*, J. Phys. Conf. Ser. **282**, 012019 (2011).
[55] O. B. Tarasov and D. Bazin, Nucl. Instrum. Methods Phys. Res., Sect. B **204**, 174 (2003).
[56] B. P. Ajith Kumar *et al.*, CANDLE: Collection and Analysis of Nuclear Data using Linux nEtwork, DAE SNP, Kolkata, 2001 (Private communication).
[57] U. Gupta *et al.*, Nucl. Phys. A **811**, 77 (2008); Phys. Rev. C **80**, 024613 (2009).
[58] E. Browne and R. B. Firestone, *Table of Radioactive Isotopes* (Wiley, New York, 1986).
[59] V. R. Sharma *et al.*, Phys. Rev. C **84**, 014612 (2011).
[60] S. F. Mughabghab, M. Divadeenam, and N. E. Holden, in *Neutron Cross-Sections*, Vol. 1 (Academic, New York, 1981), Part A, p. 89.
[61] *Table of Isotopes*, 8th ed., edited by R. B. Firestone and V. S. Shirley (Wiley, New York, 1996).
[62] B. P. Singh, M. G. V. Sankaracharyulu, M. A. Ansari, H. D. Bhardwaj, and R. Prasad, Phys. Rev. C **47**, 2055 (1993).
[63] H. Morgenstern, W. Bohne, W. Galster, and K. Grabisch, Z. Phys. A. Atomic Nuclei **324**, 443 (1986).
[64] B. S. Tomar, A. Goswami, G. K. Gubbi, A. V. R. Reddy, S. B. Manohar, B. John, and S. K. Kataria, Phys. Rev. C **58**, 3478 (1998).
[65] R. Bass, Nucl. Phys. A **231**, 45 (1974).
[66] F. D. Becchetti and G. W. Greenlees, Phys. Rev. **182**, 1190 (1969).
[67] P. M. Endt, At. Data Nucl. Data Tables **26**, 47 (1981).
[68] M. Cavinato, E. Fabrici, E. Gadioli, E. Gadioli Erba, P. Vergani, M. Crippa, G. Colombo, I. Redaelli, and M. Ripamonti, Phys. Rev. C **52**, 2577 (1995).
[69] D. P. Singh, Unnati, P. P. Singh, A. Yadav, M. K. Sharma, B. P. Singh, K. S. Golda, R. Kumar, A. K. Sinha, and R. Prasad, Phys. Rev. C **81**, 054607 (2010).
[70] P. P. Singh, M. K. Sharma, Unnati, D. P. Singh, R. Kumar, K. S. Golda, B. P. Singh, and R. Prasad, Euro. Phys. J. A **34**, 29 (2007).
[71] H. Morgenstern, W. Bohne, W. Galster, K. Grabisch, A. Kyanowski, Phys. Rev. Lett. **52**, 1104 (1984).
[72] H. Morgenstern, W. Bohne, W. Galster, K. Grabisch, and A. Kyanowski, Z. Phys. A **313**, 39 (1983); H. M. Morgenstern, W. Bohne, K. Grabisch, D. G. Kovar, and H. Lehr, Phys. Lett. B **113**, 463 (1982).
[73] M. K. Sharma, Unnati, B. P. Singh, R. Kumar, K. S. Golda, H. D. Bhardwaj, and R. Prasad, Nucl. Phys. A **776**, 83 (2006).
[74] J. Wilczynski *et al.*, Phys. Rev. Lett. **45**, 606 (1980).
[75] K. Hagino, N. Rowley, and A. T. Kruppa, Comput. Phys. Commun. **123**, 143 (1999).
[76] A. Yadav, V. R. Sharma, P. P. Singh, D. P. Singh, R. Kumar, Unnati, M. K. Sharma, B. P. Singh, R. Prasad, and R. K. Bhowmik, Phys. Rev. C **85**, 064617 (2012), and references therein.